*Iranian Journal of Materials Science and Engineering, Vol. 18, Number 4, December 2021*
RESEARCH PAPER

# Surface Modification of the $SnO_2$ Layer Using UV-Ozone in a Perovskite Solar Cell with a Planar Structure

**Razieh Keshtmand, Mohammad R. Zamani-Meymian***

* *r_zamani@iust.ac.ir*

Department of Physics, Iran University of Science and Technology, Tehran, Iran.

**Received: August 2021** **Revised: September 2021** **Accepted: October 2021**
***DOI: 10.22068/ijmse.2394***

***Abstract:*** *Tin oxide ($SnO_2$) is used as an electron transport layer (ETL) in perovskite solar cells with a planar structure due to its good transparency and energy level alignment with the perovskite layer. The modification interface of the electron transport layer and the perovskite absorber layer plays an important role in the efficient charge extraction process at the interface. In this study, planar perovskite solar cells with configuration (FTO/$SnO_2$/mixed-cation perovskite/$CuInS_2$/Au) were prepared to investigate the effect of UV-Ozone (UVO) treated $SnO_2$ as ETL on the performance of devices. ETL treatment was performed at different times (0 to 60 min). It is shown that surface wetting was improved by UVO treating the $SnO_2$ films prior to deposition of the perovskite layer. The latter improves the contact between the ETL and the perovskite layer, allowing more efficient electron transport at the interface. Contact angle, SEM, photoluminescence spectra, and the current density-voltage tests were conducted to characterize the photovoltaic of the cells. The best PSC performance with a power conversion efficiency of 10.96% was achieved using UVO-treated $SnO_2$ ETL for 30 min, whereas the power conversion efficiency of the perovskite solar cells with $SnO_2$ ETL without UVO treatment was only 4.34%.*

**Keywords:** *$SnO_2$, UV-Ozone, treatment, planar perovskite solar cell.*

## 1. INTRODUCTION

Perovskite solar cells (PSCs) have attracted the attention of many researchers around the world due to their rapid development and high efficiency, as well as a simple and low-cost synthesis [1, 2]. At present, the planar structure is one of the most important perovskite solar cell architectures. In a typical planar PSC, an absorber layer is sandwiched between two contacts that can inject and extract electrons and holes called the electron transport layer (ETL) and hole transport layer (HTL) respectively [3]. The ETL layer plays an important role in the planar solar cell by transferring electrons from the adsorbent layer to the electrode, which also acts as a hole blocking layer to prevent charge recombination [4]. $TiO_2$ is frequently used as ETL material for PSCs which require a high temperature sintering process [5]. To further reduce the manufacturing cost and to be compatible with flexible and temperature-sensitive substrates, low temperature solution-processed ETLs are proposed [6, 7]. For planar PSCs, $SnO_2$ is a suitable candidate as an ETL by low temperature process. It has much higher electron mobility than $TiO_2$ and also has excellent optical properties, wide band gap, high transparency, and good stability [8]. However, $SnO_2$ ETL suffers from some restraints for further use in PSCs [3, 9, 10]. According to reports, the poor quality of $SnO_2$ film was produced by simple hydrolysis [11]. One of the strategies used to modify the $SnO_2$ layer is a surface treatment. So far, various surface modifications have been used to improve the wetting of $SnO_2$ films, such as Plasma [12], optical [13], and UVO [14] treatments. Among these methods, UVO treatment is considered because it is cost-effective and does not require vacuum environments [15]. This treatment is also suitable for gases, solutions, and solvents at room temperature as well as for heat unstable materials [15].

High temperature sintering is commonly applied to remove organic groups, which leads to defects in the $SnO_2$ film. As a result, prior to perovskite deposition, UVO treatment of the $SnO_2$ layer coated at low temperature is required to remove residual solvents from the $SnO_2$ surface [16]. Wetting of ETL due to UVO treatment aids in the production of a perovskite layer with decreased roughness and improved surface coverage in planar PSCs [8, 17]. In UVO treatment, ultraviolet light is produced simultaneously at two wavelengths of 253.7 and 184.9 nm with energy


[ DOI: 10.22068/ijmse.2394 ]

photon energies of 472 and 647 kJ/mol, respectively [18]. Both photon energies are higher than those of Sn-Cl and O-H bonds with bond energies of 350 and 459 kJ/mol, respectively. They are also higher than the bond energy of C-C, C-H, and C-O, about 346, 411, and 358 kJ/mol, respectively [7]. Therefore, UV light can easily break these chemical bonds so that the reaction continues. UV light with a wavelength of 184.9 nm can convert $O_2$ oxygen molecules to $O_3$ active ozone molecules, which facilitates the formation of $SnO_2$, decomposition as well as oxidation of organic compounds, and the final by-product is released as carbon dioxide ($CO_2$) vapor and water ($H_2O$) [14].

In this study, a solution-based method is used for the synthesis of $SnO_2$ owing to the production process at low temperatures as well as the easy manufacturing process.

Various technologies are used to deposit of $SnO_2$ layer such as the Solution-based method [19], sputtering [20], atomic layer deposition [21], chemical bath deposition [22], and so on. Among different methods for $SnO_2$ synthesis, solution-based methods are considered owing to the low cost and do not need complicated equipment, and could be performed at ambient conditions [23]. For $SnO_2$ preparation, either $SnCl_4$, $SnCl_2$, and their hydrates $SnCl_2.2H_2O$, $SnCl_4.5H_2O$ tin precursors, or often commercial Alfa-$SnO_2$ colloid solution (Tin(IV) oxide, 15% in $H_2O$ colloidal dispersion) is employed [13, 24–27]. Solution-based methods are divided into two categories: colloidal and molecular solutions. The commercial Alfa-$SnO_2$ precursor (Tin (IV) oxide, 15% in $H_2O$ colloidal dispersion) is a well-known colloidal precursor.

In this study, we used chloride salt to synthesize $SnO_2$ as the electron transport layer. UV treatment is an important process to improve PSCs based on $SnO_2$ ETL performance, which must be optimized depending on the type of precursor. More contaminants were produced during the synthesis of $SnO_2$ as ETL with $SnCl_4.5H_2O$ salt. To improve the performance of PSCs, these contaminants should be removed. Hence, it seems that the use of UVO treatment is a suitable and urgent procedure. It can be attributed that the as-prepared $SnO_2$ films could not carry out enough hydrolysis, resulting in the unreacted salts residuals in the films. In a paper reported by Mendez et al, they used commercial Alfa $SnO_2$ nanoparticle colloid as ETL. Using this commercial material without UV-Ozone treatment has high efficiency, as can be seen from the results in the article. Therefore, the value of the percent change in PCE before and after treatment is not very high.

Also, it is worth noting that in our work, low-cost Copper indium disulfide (CIS) mineral nanoparticles were used as HTM, which is much cheaper than spiro-OMeTAD but reduces the efficiency to some extent. The high price of Spiro-OMeTAD as an organic material is a barrier against commercializing perovskite solar cells On the other hand, in the mentioned paper, single-cation perovskite is used, which is different from the triple-cation perovskite applied in our article in terms of energy levels. In the present study, significant differences were observed in cell performance before and after UVO treatment. It is indicated that UVO treatment of synthesized $SnO_2$ with chloride salt is required and, specifically, that UVO treatment can be systematically used in PSCs to increase solar cell performance. This is an important point that can be considered in future cells construction studies to increase the efficiency of this method.

To remove organic molecules, increase wettability and improve the surface adhesion between ETL and perovskite, UVO treated-$SnO_2$ layer was used and the effect of treatment at different exposure times was investigated. Finally, devices were fabricated with an FTO/$SnO_2$/mixed-cation perovskite/HTL/Au structure (FTO/ $SnO_2$/ mixed-cation perovskite/ HTL/ Au). Low-cost indium copper sulfide (CIS) mineral nanoparticles are used instead of spiro-OMeTAD as HTL.

## 2. MATERIALS AND METHODS

### 2.1. Materials

In this research Fluorine-doped tin oxide (FTO, NSG-Pilkington, 15 $\Omega.sq^{-1}$) was used as substrate. N, N-dimethylformamide (DMF, 99.8%), dimethylsulfoxide (DMSO, 99.9%), chlorobenzene (99.9%), ethanol (99.99%), and acetonitrile (99.9%) were supplied by the Merck Co. Tin chloride pentahydrate ($SnCl_4.5H_2O$, 98%), CsI (99%) were provided by Sigma Aldrich Co. Besides, lead (II) iodide ($PbI_2$, IRASOL), lead (II) bromide ($PbBr_2$, IRASOL), formamidinium iodide (FAI, dyesol), methylammonium bromide (MABr, IRASOl), and Copper indium disulfide



[ DOI: 10.22068/ijmse.2394 ]

nanoparticles ($CuInS_2$ (CIS), IRASOL) were used.

### 2.2. PSCs fabrication

Patterned FTO substrates were sequentially cleaned in detergent solution, deionized water, acetone, and ethanol. Then, the substrates were heated at 500°C for 30 minutes and exposed to UVO for 20 min. To produce $SnO_2$ films, $SnCl_4.5H_2O$ was dissolved in ethanol to form a solution with a concentration of 0.1 M and the precursor solution was spun on FTO substrate at 5000 rpm for 30 s in ambient conditions. Deposited $SnO_2$ films were placed over a hotplate set to 180°C for 30 min. prior to perovskite absorber layer deposition, the prepared $SnO_2$ films were treated with UVO at different times of 0, 10, 20, 30 min. The synthesis of mixed-cation perovskite $(Cs_{0.05}(MA_{0.17}FA_{0.83})_{0.95}Pb(I_{0.83}Br_{0.17})_3$ precursor solution was carried out as previously reported [19]. Generally, a precursor solution was composed by mixing $PbI_2$ (1.5 m), $PbBr_2$ (1.5 m), MABr (25 mg), and FAI (200 mg) in 1 mL of a mixed solvent of DMF/DMSO (4:1 v/v). Then, 50.6 µL of CsI solution (1 m in DMSO) was added to form a mixed cation (Cs/MA/FA) perovskite. Perovskite layers are deposited by two-step spin coating method, at 1000 and 6000 rpm for 10 and 20 s, respectively. During the last 8 s of the second step, 0.27 ml of chlorobenzene as anti-solvent was dropped on the substrates, and films were immediately annealed on a hot plate at 100°C for 60 min. CIS solution was deposited on perovskite layer by spin-coating at 3000 rpm for 30 s, followed by heating at 100°C for 10 min. This step was repeated two times. Finally, Au thin film was deposited by thermal evaporation under $2.0 \times 10^{-5}$ torr vacuum pressure. The scheme of fabrication process for the PSCs is depicted in Fig 1.

### 2.3. Characterization

The Motto-Schottky plots were obtained at 1000 Hz by using an Autolab system (Metrohm-Autolab potentiostat). The absorption spectrum was measured using a UV−Vis spectrometer (PerkinElmer, Lambda 25). Measurement of contact angle to check the hydrophilicity of the surface was performed by a system equipped with a CCD camera capable of photographing the drop and having software for measuring the contact angle of the drop with the desired surface. Photoluminescence spectroscopy (PL, excited at 405 nm) was performed with Avantes TEC 2048. Scanning electron microscopy (SEM, Vega 2 Tescan) was used to study the surface morphology of the perovskite films. The current density-voltage (J-V) curves were recorded under AM1.5 standard illumination using Palmsens potentiostat and IRASOL SIM- 1020 solar simulator.

## 3. RESULTS AND DISCUSSION

The Mott−Schottky (MS) plot (inverse square capacitance ($1/C^2$) vs applied bias (V) is performed to evaluate the flat−band potential ($V_{fb}$) and nature of the carrier type of ETLs. The measurements were conducted on the same electrochemical workstation in the standard three−electrode cell. A 0.5 M $Na_2SO_4$ aqueous solution was used as the electrolyte. The potential ranged from −0.8 to 0.4V (vs Ag/AgCl) at a fixed frequency of 1 kHz.

Fig 2a shows the MS plot of the $SnO_2$ film and FTO.

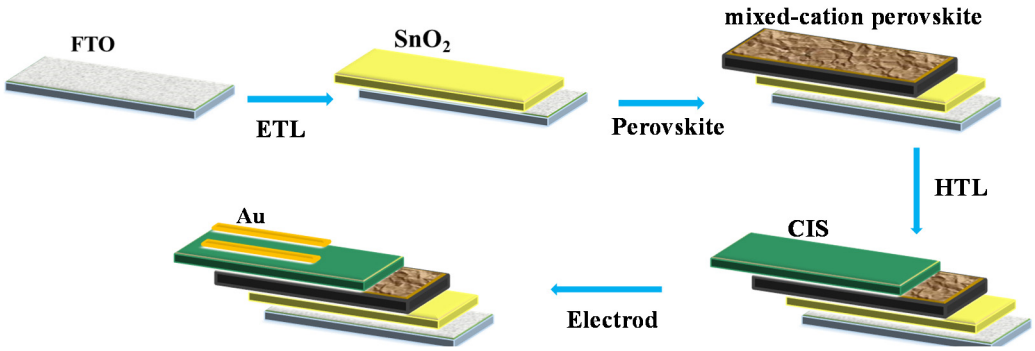


**Fig. 1.** Scheme of fabrication process for the PSCs.



[ DOI: 10.22068/ijmse.2394 ]

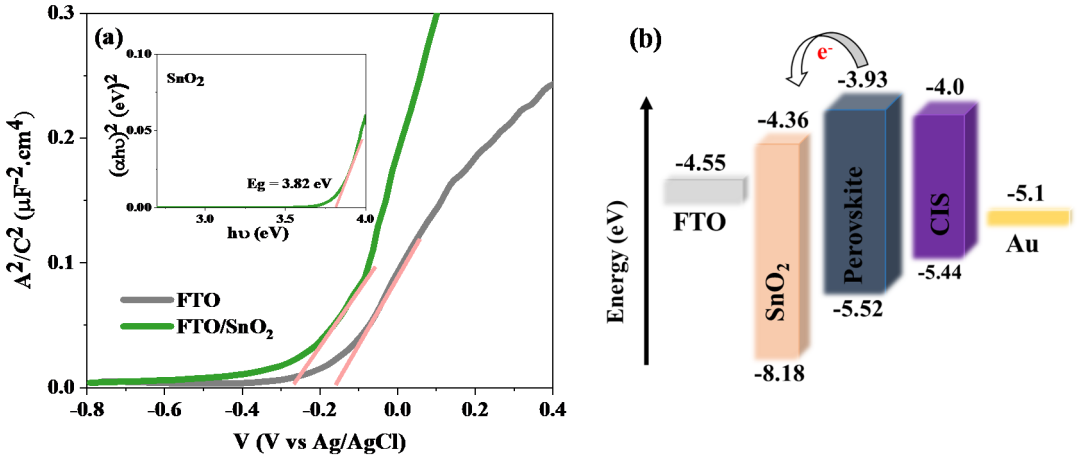


**Fig. 2.** (a) Mott-Schottky plots of FTO and $SnO_2$ spin-coated on FTO substrate, (Inset: plot of $(\alpha hv)^2$ versus hv for $SnO_2$ film), and (b) Energy level diagram of materials used in the planar PSC.

The flat band potential is determined from the intersection of the linear part of the curve with the horizontal axis. The value of the flat band potential for FTO and the $SnO_2$ layer was estimated at -4.55 and -4.44 eV, respectively. The slope of the MS curve indicates the behavior of the film; the positive slope suggests the n-type semiconductor of $SnO_2$.

Mott Schottky equation (1) is as follows:

$$1/C^2 = \frac{2}{e\varepsilon\varepsilon_0 A^2 N_D}\left(V - V_{fb} - \frac{KT}{e}\right) \quad (1)$$

Here C, A, $N_D$, V, T, K, e, ε, and ε° are interfacial capacitance, semiconductor/electrolyte interfacial area, carrier concentration, applied voltage, absolute temperature, Boltzmann constant, electronic charge, vacuum permittivity, and dielectric constant of semiconductor, respectively [20].

The absorption spectrum was measured for the $SnO_2$ layer and the direct band gap is calculated using the Tauck equation (2).

$$(\alpha hv)^2 = A(hv - E_g) \quad (2)$$

where A is a constant, Eg is the optical band gap, (hv) is incident photon energy, and α absorption coefficient [21]. The optical band gap is determined from the extrapolation of the straight-line portion of $(\alpha hv)^2$ vs hv plot (as see in the insets of Fig 2a) to the (hv) axis. The estimated band gap of the $SnO_2$ film was about 3.82 eV. In addition, combined with the UV-Vis analysis and mott Schottky the energy band structures could be calculated for $SnO_2$ film (Fig 2b). Fig 2b shows the energy levels of individual layers used in a device, which consist of a perovskite adsorbent layer, an electron transport layer ($SnO_2$), and a hole transport layer (CIS). FTO and gold (Au) have also been utilized as anode and cathode, respectively. Combined with the UV-vis analysis and Mott Schottky the energy level structures could be calculated for $SnO_2$ film (Fig 2b) [22]. The energy levels of perovskite, CIS, and Au are from the literature [23]. In In order to In order to observe the increase of surface wettability of the $SnO_2$ films after treatment with UVO, contact angle measurement was performed.

Fig 3(a-d) displays the contact angles of water droplets on UVO-treated $SnO_2$ films at different times of 0, 10, 20, and 30 min, respectively. As shown in Fig 3(a-d), contact angles decreased from 58.5° to 24.5° after 30 min of UVO treatment, which indicates the enhanced hydrophilic property of the $SnO_2$ surface. Increasing the hydrophobicity can be attributed to the active oxygen radicals generated by UVO, leading to the formation of hydroxyl groups in the Sn-O bond and replaces them with the Sn-OH hydroxide groups [15] (The OH groups formed on the surface after exposing the samples under UVO are shown in schematic Fig 3e).

Interface modification of the ETL and perovskite absorber layer has a significant impact on the surface morphology of perovskite layer. The top-view SEM images of perovskite film deposited on UVO-treated $SnO_2$ at different times are represented in Fig 4(a-d). The continuity of the $SnO_2$ films treated with UVO for 0 and 10 minutes, as shown in Fig 4 a, b, is poor, with voids and non-uniformity covering visible.



[ DOI: 10.22068/ijmse.2394 ]

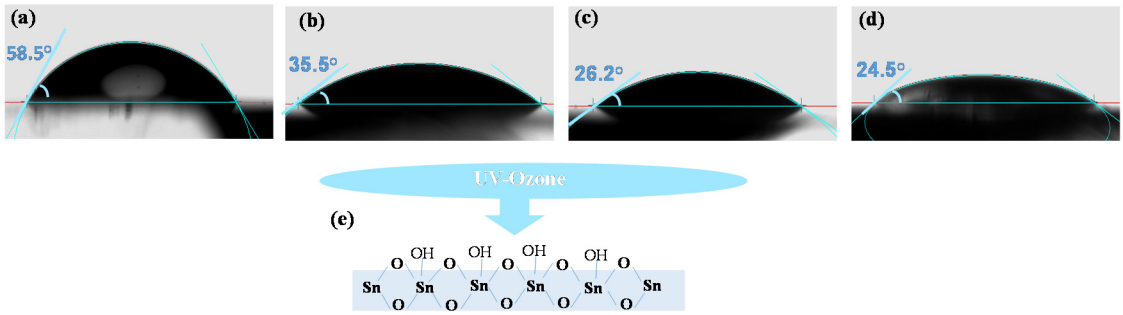


**Fig. 3.** The contact angle of $SnO_2$ thin films at different UVO exposure times: (a) 0 min, (b) 10 min, (c) 20 min, (d) 30 min, and (e) a schematic illustration of surface hydroxyl groups after UVO treatment.

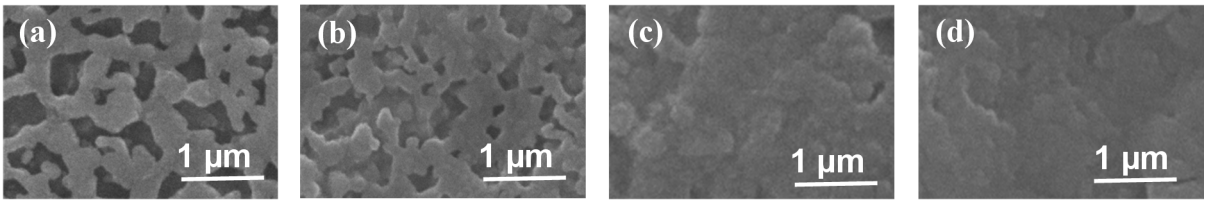


**Fig. 4.** Top-view SEM images of perovskite films deposited on $SnO_2$ layer at different UVO exposure times: (a) 0 min (b) 10 min, (c) 20 min, and (d) 30 min.

These non uniformity causes cracks between the ETL and HTL layers, which generates recombination centers and negatively impacting PSC performance. It was found that as the UVO treatment time increased, pinhole and crack-free thin films were formed (Fig 4 c, d).

To investigate the effect of the UVO-treated $SnO_2$ ETL on the performance of planar PSCs, devices with structure (FTO/$SnO_2$/mixed-cation perovskite/CIS/Au) were prepared. The current density–voltage (J-V) curves and photovoltaic characteristics are illustrated in Fig 5a and Table 1. As shown in Table 1, the device based on optimized UVO-treated $SnO_2$ for 30 min exhibited the highest power conversion efficiency (PCE) of 10.94% with a fill factor (FF) of 58.3%, an open-circuit voltage (VOC) of 0.93 V, and a short circuit current density (JSC) of 39.9 $mA.cm^{-2}$.

It can attribute that UVO treatment enhances the interaction between the ETL and the perovskite layer, and coverage of the perovskite layer improves; thereby facilitating electron transport from the perovskite layer to the ETL. It is noteworthy that cells based on $SnO_2$ for the UVO treatment time of more than 30 min did not cause a significant change in the solar cell efficiency. Fig 5b shows photoluminescence (PL) spectra of perovskite films spin-coated on glass, glass/ UVO-treated $SnO_2$ ETL at different times (0, 10, 20, 30, 40, 50, and 60 min), respectively. All samples show a peak intensity of about 760 nm. Meanwhile, the peak position in Fig 5b displays nearly no shift. As indicated in Fig 5b, the PL intensity for glass/perovskite is higher than that of glass/ETL/perovskite, arising due to the radiative recombination.

The PL quenching for the perovskite/$SnO_2$ treated with UVO (30, 40, 50, and 60 min) samples is most efficient, implying an evaluated electron extraction ability.

Fig 5. (a) Current density-voltage curves of solar cells based on UVO-treated $SnO_2$ ETL at different times (0, 10, 20, 30, 40, 50, and 60 min), (b) The photoluminescence spectra of the perovskite layer deposited on the glass and UVO-treated $SnO_2$ layers at different times (0, 10, 20, 30, 40, 50, and 60 min).

The main parameters that are applied to characterize the performance of solar cells are listed in Table 1. The results show that the best treatment time is 30 minutes. During this time, improving the wettability of the $SnO_2$ film provided better contact at the ETL/perovskite interface, suppressed recombination process, and improved electron injection at the interface [24]. The following are the consequences of UVO treatment: 1) to improve the perovskite layer wettability, and 2) to passivate the Surface of ETL by reducing the recombination centers (see PL test) and enhancing the Jsc, which is consistent with reported results by Mendez et al. [15].



[ DOI: 10.22068/ijmse.2394 ]

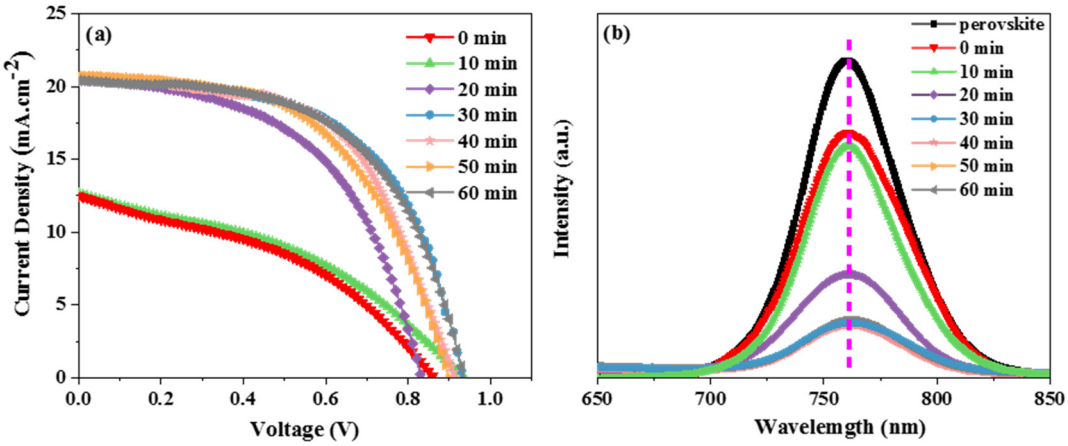


**Fig. 5.** . (a) Current density-voltage curves of solar cells based on UVO-treated $SnO_2$ ETL at different times (0, 10, 20, 30, 40, 50, and 60 min), (b) The photoluminescence spectra of the perovskite layer deposited on the glass and UVO-treated $SnO_2$ layers at different times (0, 10, 20, 30, 40, 50, and 60 min).

**Table 1.** Photovoltaic parameters of devices based on UVO-treated $SnO_2$ films at different times.

| UVO-$SnO_2$ time | $J_{SC}$ (mA.cm$^{-2}$) | $V_{OC}$ (V) | FF (%) | PCE (%) |
|---|---|---|---|---|
| 0 min | 12.20 | 0.86 | 41.1 | 4.34 |
| 10 min | 12.38 | 0.93 | 40.0 | 4.61 |
| 20 min | 20.32 | 0.83 | 53.8 | 9.07 |
| 30 min | 20.39 | 0.92 | 58.3 | 10.96 |
| 40 min | 20.72 | 0.91 | 56.1 | 10.51 |
| 50 min | 20.69 | 0.90 | 58.1 | 10.81 |
| 60 min | 20.40 | 0.93 | 57.0 | 10.81 |

It is worth noting that UV treatment of as-prepared $SnO_2$ films$_2$ as ETL, the precursors obtained from the chloride salts, was an essential step before the perovskite deposition. The principal purpose of performing this treatment was to clean up the surface of the substrates from volatile organic compounds as well as the enhancement of wettability. Also, the PCE histogram for UVO treated $SnO_2$ films at different times is plotted in Fig 6a (7 samples for each condition).

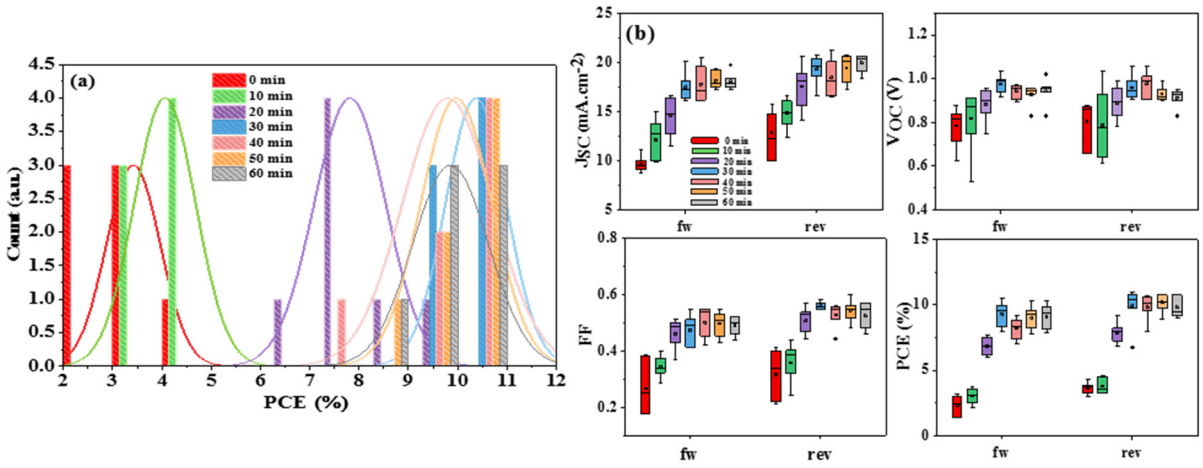


**Fig. 6.** (a) Histogram of PCE and (b) Box plots of the photovoltaic parameters ($J_{SC}$, $V_{OC}$, FF, and PCE) for forward potential scan (fw) and reverse potential scan (rev) of devices based on UVO-treated $SnO_2$ at different times (0, 10, 20, 30, 40, 50, and 60 min).



[ DOI: 10.22068/ijmse.2394 ]

Due to the distribution of data, the device based on UVO-treated $SnO_2$ film for 30 minutes has the maximum efficiency and reproducibility, which agrees to the treatment impact of UVO on $SnO_2$ film and the ETL/perovskite interface mentioned above. Fig 6b shows photovoltaic parameters measured by the reverse and forward scan for 7 different devices fabricated. Interestingly, hysteresis was observed for devices without UV-Ozone, where the parameters measured during reverse scan were larger than the ones measured during the forward scan. To quantify the extent of hysteresis, a hysteresis factor (HF) is introduced $HF = \frac{PCE_{reverse} - PCE_{forward}}{PCCE_{reverse}}$ [34]. The calculated HF for the best solar cells based on treated $SnO_2$ by UVO for 0, 10, 20, 30, 40, 50, and 60 min are 0.58, 051, 0.32, 0.24, 0.22, 0.23 and 0.22, respectively. The hysteresis for the treated solar cell is improved with increasing UVO exposure time.

## 4. CONCLUSIONS

In summary, the performance of planar PSCs was modified by the UVO treatment on the SnO2 ETLs at different times. The optimal treatment time was determined as 30 min. The characterization results showed that by increasing the UVO exposure time (30 min), $SnO_2$ film became more hydrophilic, with a contact angle of 24.5°, evidencing the removal of organic residue related to the precursor reagents from the surface of $SnO_2$ film.

Results of PL spectra indicated a better electron transfer at the interface by UVO treatment which is associated with good contact between ETL and perovskite layer. Finally, devices were prepared with the structure of (FTO/$SnO_2$/mixed-cation perovskite/CIS/Au), and for the device based on UVO (30 min) - treated $SnO_2$ ETL a maximum PCE of 10.96% was achieved.

The result which is significantly higher than that of a device based on $SnO_2$ ETL without UVO treatment (4.34%).

## 5. ACKNOWLEDGMENT

We gratefully acknowledge the partial support of this work from the Research Council of the Iran University of Science and Technology. Also, we thank the members of the nanoparticles and coating Laboratory (NCL) of the Sharif University of Technology for their useful help in this work.

## 6. REFERENCES

[1] M.C. Wu, S.H. Chan, K.M. Lee, S.H. Chen, M.H. Jao, Y.F. Chen, W.F. Su, Enhancing the efficiency of perovskite solar cells using mesoscopic zinc-doped $TiO_2$ as the electron extraction layer through band alignment, J. Mater. Chem. A. 6 (2018) 16920–16931. https://doi.org/10.1039/c8ta05291c.

[2] C. Gong, S. Tong, K. Huang, H. Li, H. Huang, J. Zhang, J. Yang, Flexible Planar Heterojunction Perovskite Solar Cells Fabricated via Sequential Roll-to-Roll Microgravure Printing and Slot-Die Coating Deposition, Sol. RRL. 4 (2020) 1–9. https://doi.org/10.1002/solr.201900204.

[3] G. Yang, C. Wang, H. Lei, X. Zheng, P. Qin, L. Xiong, X. Zhao, Y. Yan, G. Fang, Interface engineering in planar perovskite solar cells: Energy level alignment, perovskite morphology control and high performance achievement, J. Mater. Chem. A. 5 (2017) 1658–1666. https://doi.org/10.1039/c6ta08783c.

[4] N. Zhou, Q. Cheng, L. Li, H. Zhou, Doping effects in $SnO_2$ transport material for high performance planar perovskite solar cells, J. Phys. D. Appl. Phys. 51 (2018). https://doi.org/10.1088/1361-6463/aad685.

[5] M. Singh, A. Ng, Z. Ren, H. Hu, H.C. Lin, C.W. Chu, G. Li, Facile synthesis of composite tin oxide nanostructures for high-performance planar perovskite solar cells, Nano Energy. 60 (2019) 275–284. https://doi.org/10.1016/j.nanoen.2019.03.044.

[6] P. Shen, M. Yao, G. Wang, R. Mi, W. Guo, Y. Bai, L. Shen, High-efficiency polymer solar cells with low temperature solution-processed $SnO_2$/PFN as a dual-function electron transporting layer, J. Mater. Chem. A. 6 (2018) 17401–17408. https://doi.org/10.1039/c8ta06378h.

[7] F. Li, M. Xu, X. Ma, L. Shen, L. Zhu, Y. Weng, G. Yue, F. Tan, C. Chen, UV Treatment of Low-Temperature Processed $SnO_2$ Electron Transport Layers for Planar



[ DOI: 10.22068/ijmse.2394 ]

Perovskite Solar Cells, Nanoscale Res. Lett. 13 (2018). https://doi.org/10.1186/s11671-018-2633-z.

[8] W.Q. Wu, D. Chen, R.A. Caruso, Y.B. Cheng, Recent progress in hybrid perovskite solar cells based on n-type materials, J. Mater. Chem. A. 5 (2017) 10092–10109. https://doi.org/10.1039/c7ta02376f.

[9] J. Ye, Y. Li, A.A. Medjahed, S. Pouget, D. Aldakov, Y. Liu, P. Reiss, Doped Bilayer Tin (IV) Oxide Electron Transport Layer for High Open-Circuit Voltage Planar Perovskite Solar Cells with Reduced Hysteresis, Small. 17 (2021) 1–9. https://doi.org/10.1002/smll.202005671.

[10] J. Wang, K. Datta, C.H.L. Weijtens, M.M. Wienk, R.A.J. Janssen, Insights into Fullerene Passivation of $SnO_2$ Electron Transport Layers in Perovskite Solar Cells, Adv. Funct. Mater. 29 (2019). https://doi.org/10.1002/adfm.201905883.

[11] G. Murugadoss, H. Kanda, S. Tanaka, H. Nishino, S. Ito, H. Imahoric, T. Umeyama, An efficient electron transport material of tin oxide for planar structure perovskite solar cells, J. Power Sources. 307 (2016) 891–897, https://doi.org/10.1016/j.jpowsour.2016.01.044.

[12] Y. Luan, X. Yi, P. Mao, Y. Wei, J. Zhuang, N. Chen, T. Lin, C. Li, J. Wang, High-Performance Planar Perovskite Solar Cells with Negligible Hysteresis Using 2, 2, 2-Trifluoroethanol-Incorporated $SnO_2$, IScience. 16 (2019) 433–441. https://doi.org/10.1016/j.isci.2019.06.004.

[13] M. Zhu, W. Liu, W. Ke, S. Clark, E.B. Secor, T. Bin Song, M.G. Kanatzidis, X. Li, M.C. Hersam, Millisecond-pulsed photonically-annealed tin oxide electron transport layers for efficient perovskite solar cells, J. Mater. Chem. A. 5 (2017) 24110–24115, https://doi.org/10.1039/c7ta07969a.

[14] L. Huang, X. Sun, C. Li, J. Xu, R. Xu, Y. Du, J. Ni, H. Cai, J. Li, Z. Hu, J. Zhang, UV-Sintered Low-Temperature Solution-Processed $SnO_2$ as Robust Electron Transport Layer for Efficient Planar Heterojunction Perovskite Solar Cells, ACS Appl. Mater. Interfaces. 9 (2017) 21909–21920. https://doi.org/10.1021/acsami.7b04392.

[15] P.F. Méndez, S.K.M. Muhammed, E.M. Barea, S. Masi, I. Mora-Seró, Analysis of the UV–Ozone-Treated $SnO_2$ Electron Transporting Layer in Planar Perovskite Solar Cells for High Performance and Reduced Hysteresis, Sol. RRL. 3 (2019) 1–10. https://doi.org/10.1002/solr.201900191.

[16] H. Liu, Z. Chen, H. Wang, F. Ye, J. Ma, X. Zheng, P. Gui, L. Xiong, J. Wen, G. Fang, A facile room temperature solution synthesis of $SnO_2$ quantum dots for perovskite solar cells, J. Mater. Chem. A. 7 (2019) 10636–10643. https://doi.org/10.1039/c8ta12561a.

[17] X. Li, S.M. Dai, P. Zhu, L.L. Deng, S.Y. Xie, Q. Cui, H. Chen, N. Wang, H. Lin, Efficient Perovskite Solar Cells Depending on $TiO_2$ Nanorod Arrays, ACS Appl. Mater. Interfaces. 8 (2016) 21358–21365. https://doi.org/10.1021/acsami.6b05971.

[18] P. Kuang, K. Constant, Increased Wettability and Surface Free Energy of Polyurethane by Ultraviolet Ozone Treatment, Wetting and Wettability. (2015). https://doi.org/10.5772/60798.

[19] L. Xiong, M. Qin, G. Yang, Y. Guo, H. Lei, Q. Liu, W. Ke, H. Tao, P. Qin, S. Li, H. Yu, G. Fang, Performance enhancement of high temperature $SnO_2$-based planar perovskite solar cells: Electrical characterization and understanding of the mechanism, J. Mater. Chem. A. 4 (2016) 8374–8383. https://doi.org/10.1039/c6ta01839d.

[20] L. Qiu, Z. Liu, L.K. Ono, Y. Jiang, D.Y. Son, Z. Hawash, S. He, Y. Qi, Scalable Fabrication of Stable High Efficiency Perovskite Solar Cells and Modules Utilizing Room Temperature Sputtered $SnO_2$ Electron Transport Layer, Adv. Funct. Mater. 29 (2019). https://doi.org/10.1002/adfm.201806779.

[21] Y. Lee, S. Lee, G. Seo, S. Paek, K.T. Cho, A.J. Huckaba, M. Calizzi, D. won Choi, J.S. Park, D. Lee, H.J. Lee, A.M. Asiri, M.K. Nazeeruddin, Efficient Planar Perovskite Solar Cells Using Passivated Tin Oxide as an Electron Transport Layer, Adv. Sci. 5 (2018) 1–6. https://doi.org/10.1002/advs.201800130.



[ DOI: 10.22068/ijmse.2394 ]

[22] Y. Ko, Y. Kim, C. Lee, T. Kim, S. Kim, Y.J. Yun, H. jeong Gwon, N.H. Lee, Y. Jun, Self-Aggregation-Controlled Rapid Chemical Bath Deposition of $SnO_2$ Layers and Stable Dark Depolarization Process for Highly Efficient Planar Perovskite Solar Cells, ChemSusChem. 13 (2020) 4051–4063. https://doi.org/10.1002/cssc.202000501.

[23] B.G. Pawar, D. V. Pinjari, S.S. Kolekar, A.B. Pandit, S.H. Han, Effect of Sintering Temperatures on the Synthesis of $SnO_2$ Nanospheres, ISRN Chem. Eng. 2012 (2012) 1–7. https://doi.org/10.5402/2012/954869.

[24] H. Ye, Z. Liu, X. Liu, B. Sun, X. Tan, Y. Tu, T. Shi, Z. Tang, G. Liao, 17.78% efficient low-temperature carbon-based planar perovskite solar cells using Zn-doped $SnO_2$ electron transport layer, Appl. Surf. Sci. 478 (2019) 417–425. https://doi.org/10.1016/j.apsusc.2019.01.237.

[25] Z. Xu, S.H. Teo, L. Gao, Z. Guo, Y. Kamata, S. Hayase, T. Ma, La-doped $SnO_2$ as ETL for efficient planar-structure hybrid perovskite solar cells, Org. Electron. 73 (2019) 62–68. https://doi.org/10.1016/j.orgel.2019.03.053.

[26] C. Wang, C. Zhang, S. Wang, G. Liu, H. Xia, S. Tong, J. He, D. Niu, C. Zhou, K. Ding, Y. Gao, J. Yang, Low-Temperature Processed, Efficient, and Highly Reproducible Cesium-Doped Triple Cation Perovskite Planar Heterojunction Solar Cells, Sol. RRL. 2 (2018) 1700209. https://doi.org/10.1002/solr.201700209.

[27] S.S. Shin, W.S. Yang, J.H. Noh, J.H. Suk, N.J. Jeon, J.H. Park, J.S. Kim, W.M. Seong, S. Il Seok, High-performance flexible perovskite solar cells exploiting $Zn_2SnO_4$ prepared in solution below 100°C, Nat. Commun. 6 (2015) 1–8. https://doi.org/10.1038/ncomms8410.

[28] F. Behrouznejad, M. Forouzandeh, R. Khosroshahi, K. Meraji, M.N. Badrabadi, M. Dehghani, X. Li, Y. Zhan, Y. Liao, Z. Ning, N. Taghavinia, Effective Carbon Composite Electrode for Low-Cost Perovskite Solar Cell with Inorganic $CuIn_{0.75}Ga_{0.25}S_2$ Hole Transport Material, Sol. RRL. 4 (2020) 1–11. https://doi.org/10.1002/solr.201900564.

[29] L. Wang, X. Gu, Y. Zhao, Y. Qiang, C. Huang, J. Song, Preparation of ZnO/ZnS thin films for enhancing the photoelectrochemical performance of ZnO, Vacuum. 148 (2018) 201–205. https://doi.org/10.1016/j.vacuum.2017.11.023.

[30] D.A. Granada-Ramirez, J.S. Arias-Cerón, M.L. Gómez-Herrera, J.P. Luna-Arias, M. Pérez-González, S.A. Tomás, P. Rodríguez-Fragoso, J.G. Mendoza-Alvarez, Effect of the indium myristate precursor concentration on the structural, optical, chemical surface, and electronic properties of InP quantum dots passivated with ZnS, J. Mater. Sci. Mater. Electron. 30 (2019) 4885–4894. https://doi.org/10.1007/s10854-019-00783-6.

[31] C. Chen, Y. Peng, M. Lin, K. Chang, Y. Lin, J. Sun, Iron Modified Titanate Nanotube Arrays for Photoelectrochemical Removal of E . coli, (2021).

[32] A. Khorasani, M. Marandi, R. Khosroshahi, M. Malekshahi Byranvand, M. Dehghani, A.I. Zad, F. Tajabadi, N. Taghavinia, Optimization of $CuIn_1$-$XGaXS_2$ Nanoparticles and Their Application in the Hole-Transporting Layer of Highly Efficient and Stable Mixed-Halide Perovskite Solar Cells, ACS Appl. Mater. Interfaces. 11 (2019) 30838–30845. https://doi.org/10.1021/acsami.9b08714.

[33] J. Du, L. Feng, X. Guo, X. Huang, Z. Lin, J. Su, Z. Hu, J. Zhang, J. Chang, Y. Hao, Enhanced efficiency and stability of planar perovskite solar cells by introducing amino acid to $SnO_2$ / perovskite interface, 455 (2020).

[34] R. Keshtmand, M.R. Zamani-Meymian, F. Mohamadkhani, N. Taghavinia, Smoothing and coverage improvement of $SnO_2$ electron transporting layer by NH4F treatment: Enhanced fill factor and efficiency of perovskite solar cells, Sol. Energy. 228 (2021) 253–262. https://doi.org/10.1016/j.solener.2021.09.068.



[ DOI: 10.22068/ijmse.2394 ]